J Incl Phenom Macrocycl Chem (2010) 66:87–94
DOI 10.1007/s10847-009-9648-0

ORIGINAL ARTICLE

Thiazole-based chemosensor II: synthesis and fluorescence sensing of fluoride ions based on inhibition of ESIPT

Aasif Helal · Nugen Thi Thu Thao · Soon W. Lee · Hong-Seok Kim

Received: 1 July 2009 / Accepted: 12 July 2009 / Published online: 1 August 2009

Abstract Novel chemosensors based on 2-(2′-hydroxyphenyl)-4-phenylthiazole were synthesized and their anion sensing behaviors were investigated. Sensors **1** and **2** show fluoride ion selective behaviors related to their absorption and emission spectra amongst F^-, $CH_3CO_2^-$, $H_2PO_4^-$, Cl^-, Br^-, I^-, ClO_4^-, NO_3^-, and HSO_4^- anions. Sensor **2** shows color change upon interaction with F^-. Interactions of **1**, **2** and **3** with F^- cause a red-shift in UV–vis absorption and a large Stokes shift in fluorescence emission due to the inhibition of ESIPT induced by the deprotonation of phenolic proton by F^-.

Keywords Thiazole · Fluorescence · ESIPT · Fluoride ions · Stokes' shift

Introduction

Considerable attention has been focused on the design of chemosensors for the detection of biologically relevant anions [1–4]. In particular, selective sensing of fluoride ion has gained attention due to its significance in clinical treatment for osteoporosis and dental care [5, 6]. Recently a large number of methods for the sensing of fluoride ion have been reported [7, 8]. In biological systems fluorescence intensity is dependent on the local concentration of the sensors. However, emission intensity is also dependent on other factors, such as bleaching, optical path length, and illumination intensity. It is therefore desirable to eliminate the effects of these factors by using a ratiometric sensor that exhibits a spectral shift upon reaction or binding to the analyte of interest, so that the ratio between the two emission intensities can be used to evaluate the analyte concentration. In this respect, dual fluorescence probes exhibiting two well separated emission bands are of particular interest, since they provide a reliable ratiometric signal independent of the probe concentration [9]. Excited state intramolecular proton transfer (ESIPT) is very effective in the design of probes with dual fluorescence. ESIPT results in the formation of two tautomeric forms when the probe is in the excited state: N*-normal and T*-tautomer forms [10, 11]. ESIPT is one of the most well known photophysical processes occurring in *o*-hydroxy-benzoxazole, benzimidazole and benzothiazole [12–14]. It is expected that replacement of the oxygen atom in the oxazole ring, with a sulfur atom to form a thiazole cycle, raises molecular polarizabilities and introduces interesting novel spectral-luminescent properties. Formation of an intramolecular hydrogen bond in these compounds promotes luminescence intensity and results in abnormally large Stokes shifts that are essential for practical applications of the luminophores [6].

With reference to binding groups, only a limited number of reports are available which use –OH as a binding site [15–19]. Understanding the nature of intramolecular hydrogen bonding of phenol and fluoride ion is necessary to develop a fluoride ion selective sensor [20]. Electron-donating (CH_3) and electron-withdrawing (Br) substituents were incorporated on the *para* position of the phenol, and fluoride ion selectivity was investigated. We herein report F^- selective chemosensors possessing thiazole and a

A. Helal · N. T. T. Thao · H.-S. Kim (✉)
Department of Applied Chemistry, Kyungpook National University, Daegu 702-701, Republic of Korea
e-mail: kimhs@knu.ac.kr

S. W. Lee
Department of Chemistry and School of Molecular Science, Sungkyunkwan University, Suwon 440-746, Republic of Korea

phenolic OH group which are able to bind fluoride ions via H-bond interactions.

Experimental

Apparatus

Melting points were determined using a Thomas-Hoover capillary melting point apparatus and are uncorrected. ^{1}H and ^{13}C NMR spectra were recorded on a Bruker AM-400 spectrometer using Me_4Si as the internal standard. UV–vis absorption spectra were determined using a Shimadzu UV-1650PC spectrophotometer. Fluorescence spectra were measured using a Shimadzu RF-5301 fluorescence spectrometer equipped with a xenon discharge lamp, 1 cm quartz cells. All of the measurements were carried out at 298 K.

X-ray structure determination

All X-ray data were collected with the use of a Siemens P4 diffractometer equipped with a Mo X-ray tube. The orientation matrix and unit-cell parameters were determined by least-squares analyses of the setting angles of 33 reflections in the range $10.0° < 2\theta < 25.0°$. Intensity data were empirically corrected for absorption with ψ-scan data. All calculations were carried out with the use of SHELXTL programs [21].

Chemicals

Analytical grade acetonitrile was purchased from Merck and dried with CaH_2 before use. All other materials used for synthesis were purchased from Aldrich Chemical Co and used without further purification. 2-Hydroxythiobenzamide, 5-methyl-2-hydroxythiobenzamide, and 5-bromo-2-hydroxythiobenzamide were prepared by thionation of the corresponding salicylamide with Lawesson's reagent. In the titration experiments, all the anions were added in the form of tetrabutylammonium (TBA) salts, which were purchased from Aldrich Chemical Co., stored in a vacuum desiccator and dried fully before diluting to prepare working solutions.

Syntheses of compounds **1**, **2** and **3**

A solution of 2-hydroxythiobenzamide (1 mmol) and 2-bromoacetophenone (1 mmol) in dry EtOH (20 mL) was stirred at room temperature for 5 h. After the solvent was removed by evaporator, the mixture was extracted with CH_2Cl_2, dried over anhydrous Na_2SO_4 and evaporated. The residue was purified using SiO_2 column chromatography (elution with EtOAc in hexane) to give compound **1**.

Compound 1

Yield 84%; mp 103 °C (CH_2Cl_2-hexane); ^{1}H NMR ($CDCl_3$) δ 6.92 (dt, $J = 7.6$, 1.2 Hz, 1H), 7.12 (dd, $J = 8.3$, 1.0 Hz, 1H), 7.34 (dd, $J = 8.3$, 1.5 Hz, 1H), 7.38 (s, 1H), 7.40 (dt, $J = 8.3$, 1.2 Hz, 1H), 7.46 (dt, $J = 8.1$, 1.5 Hz, 2H), 7.65 (dd, $J = 7.8$, 1.5 Hz, 1H), 7.87 (dd, $J = 8.5$, 1.5 Hz, 2H), 12.45 (bs, OH); ^{13}C NMR ($CDCl_3$) δ 111.3, 117.1, 118.6, 119.6, 126.8, 127.6, 128.8, 129.1, 132.4, 133.2, 154.3, 157.2, 169.4; Anal. Calcd for $C_{15}H_{11}NOS$: C, 71.12; H, 4.38; N, 5.53; S, 12.66, Found: C, 70.84; H, 4.32; N, 5.46; S, 12.20.

Compound 2

Yield 95%; mp 112–114 °C (CH_2Cl_2-hexane); ^{1}H NMR ($CDCl_3$) δ 2.2 (s, 3H), 6.87 (d, $J = 8.4$ Hz, 1H), 7.01 (dd, $J = 8.4$, 2.4 Hz, 1H), 7.23 (s, 1H), 7.25-7.28 (m, 2H), 7.32 (t, $J = 8.0$ Hz, 2H), 7.73 (d, $J = 8.0$ Hz, 2H), 11.9 (bs, OH); ^{13}C NMR ($CDCl_3$) δ 20.8, 110.8, 116.7, 117.8, 119.6, 126.4, 127.3, 128.8, 129.0, 133.0, 133.4, 154.4, 154.9, 169.4; Anal. Calcd for $C_{16}H_{13}NOS$: C, 71.88; H, 4.90; N, 5.24; S, 11.99, Found C, 69.86; H, 4.87; N, 5.08; S, 11.36.

Compound 3

Yield 80%; mp 136–138 °C (CH_2Cl_2-hexane); ^{1}H NMR ($CDCl_3$) δ 6.83 (d, $J = 9.0$ Hz, 1H), 7.24–7.27 (m, 2H), 7.25 (s, 1H), 7.31 (t, $J = 7.2$ Hz, 2H), 7.55 (d, $J = 2.5$ Hz, 1H), 7.68 (d, $J = 7.6$ Hz, 2H), 12.12 (bs, OH); ^{13}C NMR ($CDCl_3$) δ 111.2, 111.6, 118.5, 119.9, 126.4, 129.0, 129.1, 129.4, 132.9, 134.6, 154.5, 156.4, 167.5; Anal. Calcd for $C_{15}H_{10}BrNOS$: C, 54.23; H, 3.03; N, 4.22; S, 9.65, Found: C, 53.88; H, 2.90; N, 4.17; S, 9.36.

Results and discussion

Synthesis

The chemosensors **1**, **2**, and **3** were synthesized in good yields by Hantzsch thiazole synthesis from the reaction of the corresponding 2-hydroxythiobenzamide and 2-bromoacetophenone as shown in Scheme 1. Initial attempts using the Hantzsch method by Bach failed to provide **1** but we succeeded in preparing the desired compounds via a simple condensation reaction [22]. The structures of chemosensors **1**–**3** were confirmed by ^{1}H, ^{13}C NMR, and elemental analyses data.

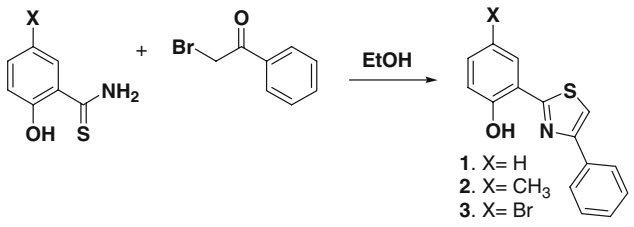

Scheme 1 Synthesis of chemosensors **1**, **2** and **3**

Crystal structure of **1**

Crystal of **1**, suitable for single crystal X-ray diffraction analysis, was obtained from dichloromethane-hexane. The molecular structure of **1** with the atom-numbering scheme is shown in Fig. 1. The overall structure is essentially planar, with dihedral angles between the central thiazole ring and the planar adjacent aryl rings, in the range of 2.3(1)–6.4(1)°. There is an intramolecular O–H···N hydrogen bonding (O1–HO1: 0.89 Å; HO1···N1: 1.83 Å; O1···N1: 2.65 Å; O1–HO1···N1 153°), whose bonding parameters indicate relatively strong hydrogen bonding.

UV–vis responses toward anions

Initial studies of the UV–vis absorption showed that **1** exhibited selectivity toward fluoride ion in CH_3CN. Figure 2a, shows the absorption spectra of **1** in CH_3CN (30 μM) upon addition of 10 equiv of tetrabutylammonium salts of these anions: F^-, $CH_3CO_2^-$, $H_2PO_4^-$, Cl^-, Br^-, I^-, ClO_4^-, NO_3^-, and HSO_4^-. Only F^- and $CH_3CO_2^-$ showed significant changes over other anions. Upon addition of fluoride ion into the **1** solution a significant red-shift ($\Delta\lambda = 68$ nm) occurred with enhancement of absorbance in the UV–vis absorption spectrum. Sensor **1** exhibited an absorption band at 332 nm (Fig. 2a), sensors **2** (Fig. 2b) and **3** (Fig. 2c) showed absorption bands at 338 and 340 nm, respectively. This may be attributed to a π–π^* charge-transfer state; which is favored by the planar orientation enforced by intramolecular hydrogen bonding [23].

Titration of **1**, as a function of F^-, revealed that the intensity of the absorption band at 332 nm decreased and a new absorption band at 400 nm appeared gradually, with an isobestic point at 353 nm (Fig. 2d). The intensity of this peak reached its maximum after the addition of 6 equiv of F^- (Fig. 2d, inset). When an excess of tetrabutylammonium salts of anions were added to sensor **1**, only F^- led to a change in λ_{max} and absorption intensity, although the addition of CH_3COO^- and $H_2PO_4^-$ produced changes in λ_{max}, their absorption intensities were very low, whereas the addition of other anions such as Cl^-, Br^-, I^-, ClO_4^-, NO_3^-, and HSO_4^- resulted in insignificant changes in the absorption spectra. In the case of sensor **2**, when excess of various anions were added to the solution (Fig. 2b), only F^- causes a red shift to 410 nm and the color of the solution changed from colorless to yellow (Fig. 3). Whereas the addition of other anions including CH_3COO^-, $H_2PO_4^-$, Cl^-, Br^-, I^-, ClO_4^-, NO_3^-, and HSO_4^- resulted in negligible changes in the absorption spectra. The color change of **2** in the CH_3CN solution can be used for naked-eye detection of F^- in the presence of other anions. In sensor **3**, when excess of anions were added (Fig. 2c), F^-, CH_3COO^- and $H_2PO_4^-$ caused a significant red shift to 410 nm whereas the addition of other anions such as Cl^-, Br^-, I^-, ClO_4^-, NO_3^- and HSO_4^- did not produce any change. These photophysical data from the chemosensors are summarized in Table 1.

The resonance structures of the deprotonated form of **1** show that the electron density of phenyl at the *para* position is increased upon deprotonation as shown in Scheme 2. This indicates that the acidity in this kind of sensor can be tuned by changing the electronic property of the substituent on the *para* position. The introduction of an electron donating methyl group at the *para* position decreases the acidity of the proton, and thus the hydrogen bonding ability is reduced. Sensor **2** can only interact with

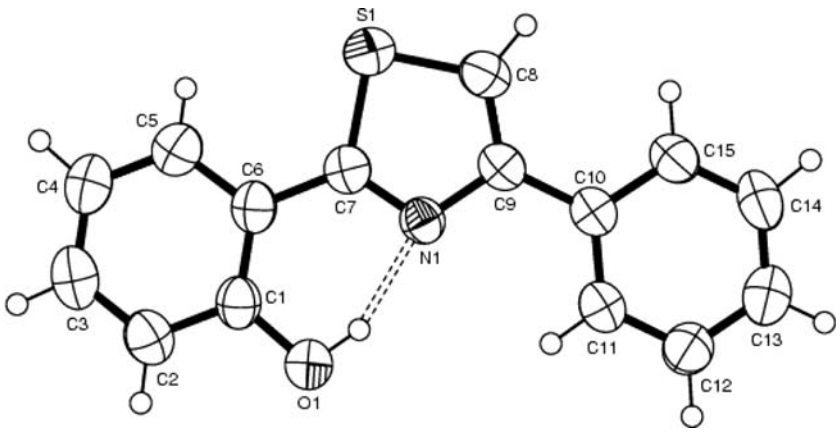

Fig. 1 ORTEP drawing of 1 with 50% probability thermal ellipsoids

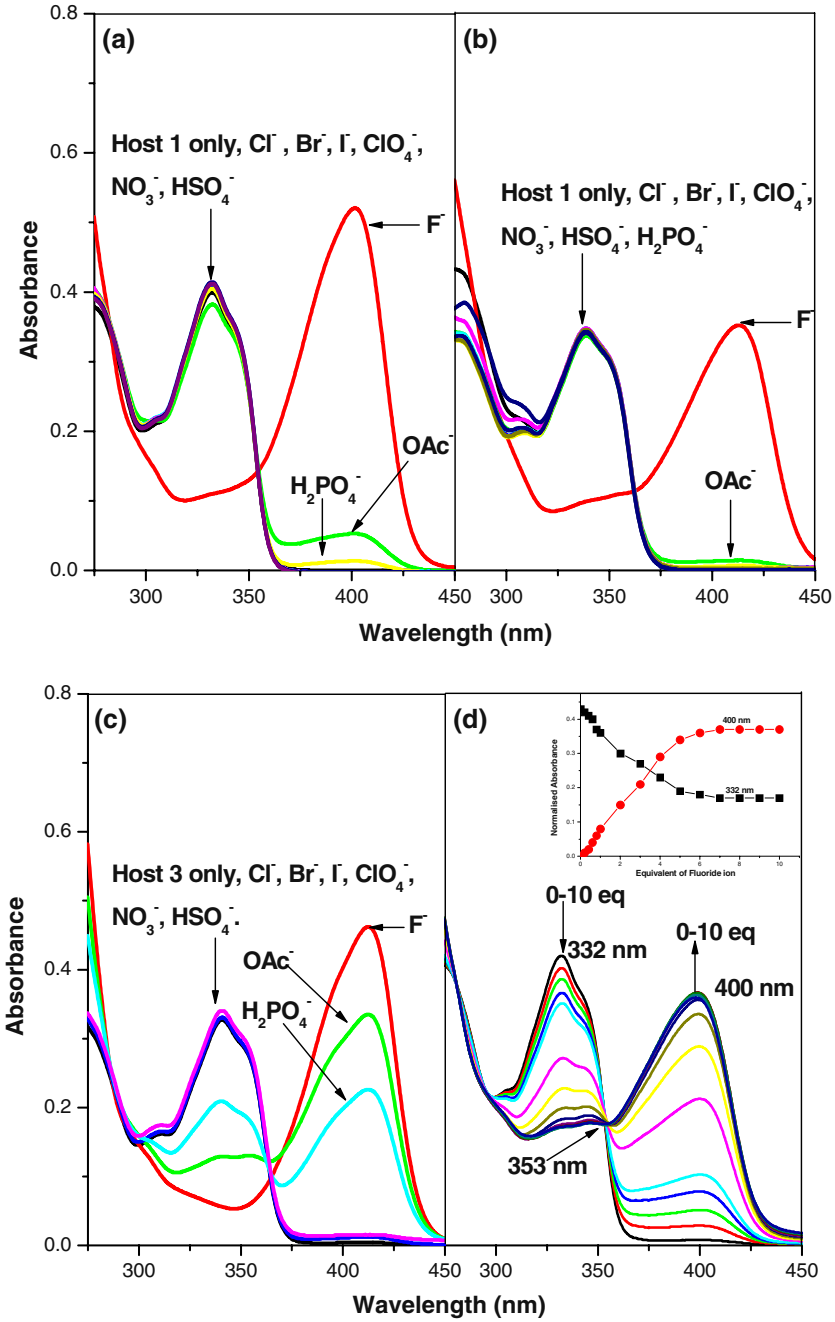

Fig. 2 UV–vis spectra of (**a**) **1** (**b**) **2** (**c**) **3** in CH_3CN (30 μM) in the presence of 10 equiv of various anions. (**d**) Changes in UV–vis spectra of **1** upon addition of $[(Bu)_4N]F$ in CH_3CN. *Inset*: mol ratio plots of absorbance at 332 and 400 nm

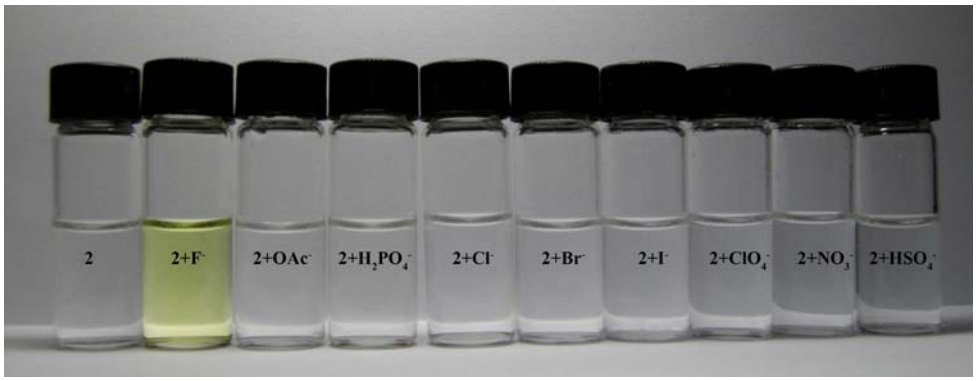

Fig. 3 Color changes of **2** in CH_3CN (50 μM) after addition of 10 equiv of representative anions

Table 1 The photophysical data of **1**, **2** and **3** in CH_3CN

Sensor	Absorption max. (nm, (log ε))			Emission max. (nm)			
	Free	With F^-	Δλ (nm)	Free (nm)		With F^-	Δλ (nm)
				N*	T*		
1	332 (3.85)	400 (3.75)	68	369	506	453	53, 84
2	338 (3.76)	410 (3.77)	78	373	525	469	56, 96
3	340 (3.76)	410 (3.89)	78	378	513	457	56, 79

*N** normal emission, *T** tautomer emission

Scheme 2 Resonance structures of **1**

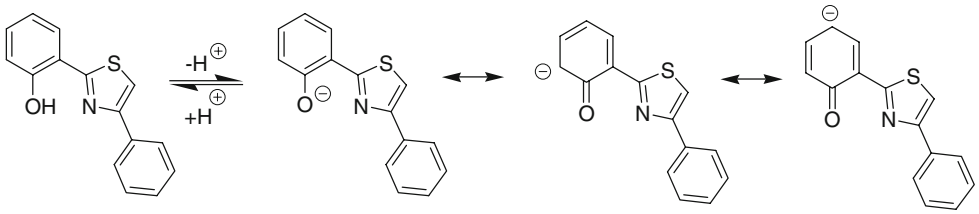

fluoride ions due to their higher electronegativity and their smaller size compared to the other halides. The presence of an electron withdrawing bromide group increases the acidity of the proton and increases the hydrogen bonding ability. Thus sensor **3** loses its selectivity toward anions.

Fluorescent responses toward anions

The fluorescence studies of **1**, **2** and **3** were performed in CH_3CN (Fig. 4). Intensities of the normal and the tautomer emissions of **1**, **2** and **3** change with the substituents at the *para* of the phenyl ring. Sensor **1**, with excitation at λ_{max} 332 nm, exhibits two emission bands at λ_{max} 369 and 506 nm. The longer wavelength emission is a typical ESIPT emission band [17]. On addition of F^- to the solution, a ratiometric change (spectral shift) occurs with the formation of a new emission band at 453 nm with the disappearance of the two emission bands of the sensor, but addition of Cl^-, Br^-, I^-, ClO_4^-, NO_3^- and HSO_4^- results in insignificant changes in the fluorescent spectra. In the case of $CH_3CO_2^-$ and $H_2PO_4^-$ anions, two new emission bands appear at 444 and 446 nm, respectively, but the intensity of the $CH_3CO_2^-$-induced band is 4 times smaller than that of F^- and the $H_2PO_4^-$-induced band is 15 times smaller.

The titration of sensor **1** with F^- revealed that the fluorescence intensity reached its maximum after addition of 6 equiv of F^- (Fig. 4a, d). In sensor **2** (Fig. 4b), the normal emission band appears at 373 nm and upon addition of F^- the emission band shifted to 469 nm and the intensity of the emission band decreased as compared to **1**. Selectivity of **2** toward F^- is the same as that of **1**. The emission band in **3** (Fig. 4c) shifted to 457 nm from the tautomer emission band (513 nm) with a sharp isoemission point at 501 nm. However its selectivity decreased as compared to **1** and **2**.

The deprotonation of the phenolic proton induced a great fluorescence enhancement due to the inhibition of ESIPT in the case of chemosensors **1**, **2**, and **3**. The emission of the deprotonated form lies just between the normal and tautomer emissions. In the case of **2**, due to the presence of the electron donating group, the normal form is more stable than the tautomer, while in sensor **3** the electron withdrawing group makes the tautomer form more stable than the normal form, but its selectivity toward anions is lost.

^{1}H NMR titration

To examine the ground state behavior of sensor **1** with fluoride ion, ^{1}H NMR experiments involving **1** with TBA^+F^- were performed in CD_3CN. Partial ^{1}H NMR spectra of **1**, with different amounts of F^-, is shown in Fig. 5. Notably, when 1 equiv of F^- was added, disappearance of phenolic proton and upfield shifts of phenyl and thiazole protons were observed. The signal of H_d shows a small upfield shift ($\Delta\delta = 0.01$ ppm) while the signals of H_a, H_b, H_c and H_e were shifted upfield significantly ($\Delta\delta = 0.08$–0.19 ppm) due to the shielding effect. Due to the deprotonation of phenolic proton, the OH proton disappeared and the *para* proton (H_c, $\Delta\delta = 0.19$ ppm) shifts upfield substantially, compared to the other phenyl protons (H_a, H_b, H_d). Theses results clearly imply that for **1**, phenolic proton strongly binds with F^- via H-bond interactions.

Binding constants

The UV and fluorescence titration studies involving the sensors indicate that the addition of 6 equiv of F^- result in the intensities of the absorption and emission bands reaching their maxima. This could be assigned as evidence for the occurrence of hydrogen bond interactions between

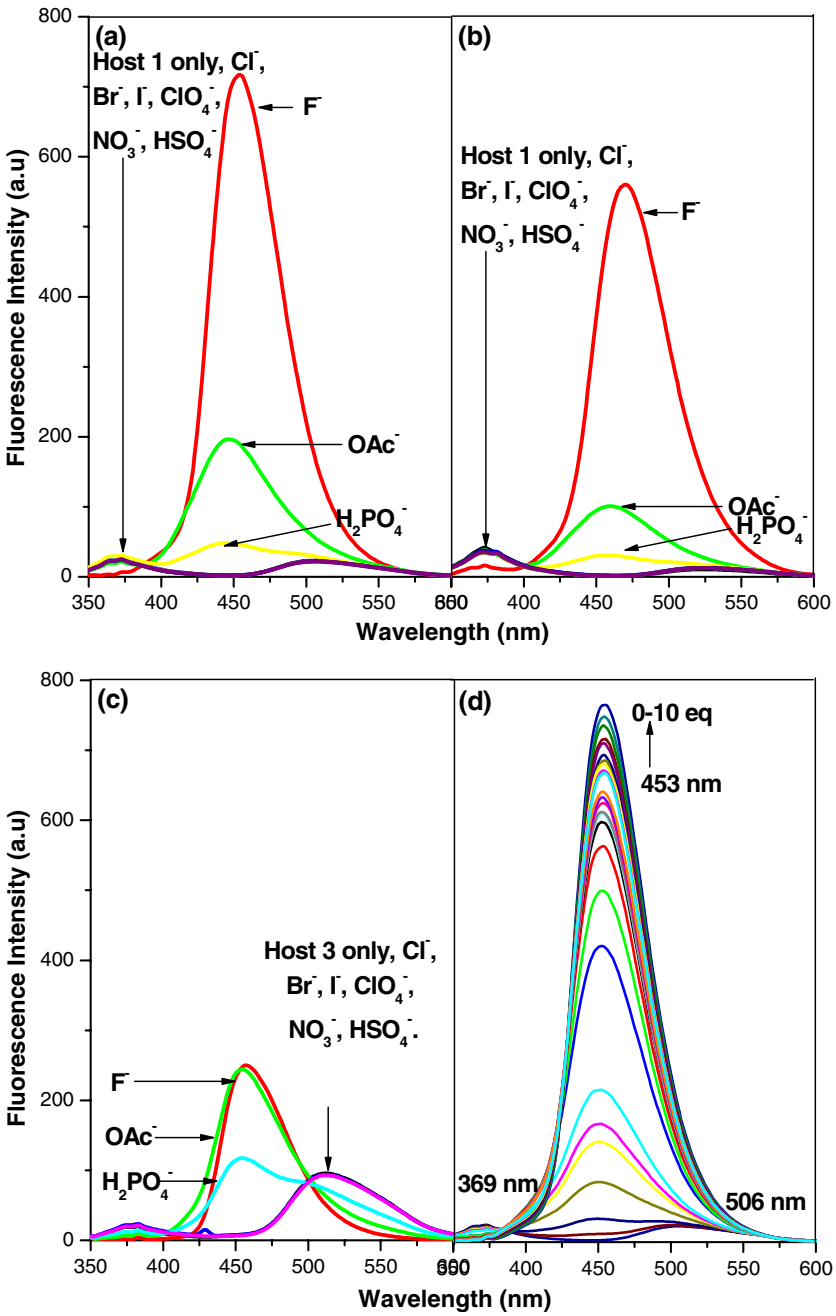

Fig. 4 Fluorescence spectra of (**a**) **1**, (**b**) **2**, (**c**) **3** in CH_3CN (30 μM) in the presence of 10 equiv of various anions with an excitation wavelength of 332, 338 and 340 nm, respectively. (**d**) Changes in fluorescent spectra of **1** in CH_3CN (30 μM) upon addition of $[(Bu)_4N]F$ excited at 332 nm

OH and F^- as shown in Scheme 3. Fluorescence based Job's plot for the complexation of **1**-F^- shows a 1:2 stoichiometry (Fig. 6).

The binding constants for the sensor-F^- complex were obtained from the variation in fluorescent intensity at an appropriate wavelength. The binding constants (*K*a) for **1**, **2**, and **3** with F^- were calculated to be 5.8×10^3, 2.1×10^3, and 8.2×10^3 M^{-1} L, respectively (Error estimated to be ≤10%). Sensor **3** shows the highest binding constant among the tested sensors. This may be due to the presence of the electron-withdrawing group, which results in strong hydrogen bond interactions with F^- as compared to **1** and **2**. Moreover the hydrogen bonding of F^-, reinforces the electron-withdrawing character of the bromo group, thus increasing the extinction coefficient. Sensor **3** also showed binding affinity toward OAc^- and $H_2PO_4^-$ with binding constants 2.0×10^3 and 1.2×10^3 M^{-1} L, respectively (Error estimated to be ≤10%).

Conclusion

In summary, new ratiometric ESIPT-chemosensors based on 2-hydroxyphenyl-thiazole have been developed for

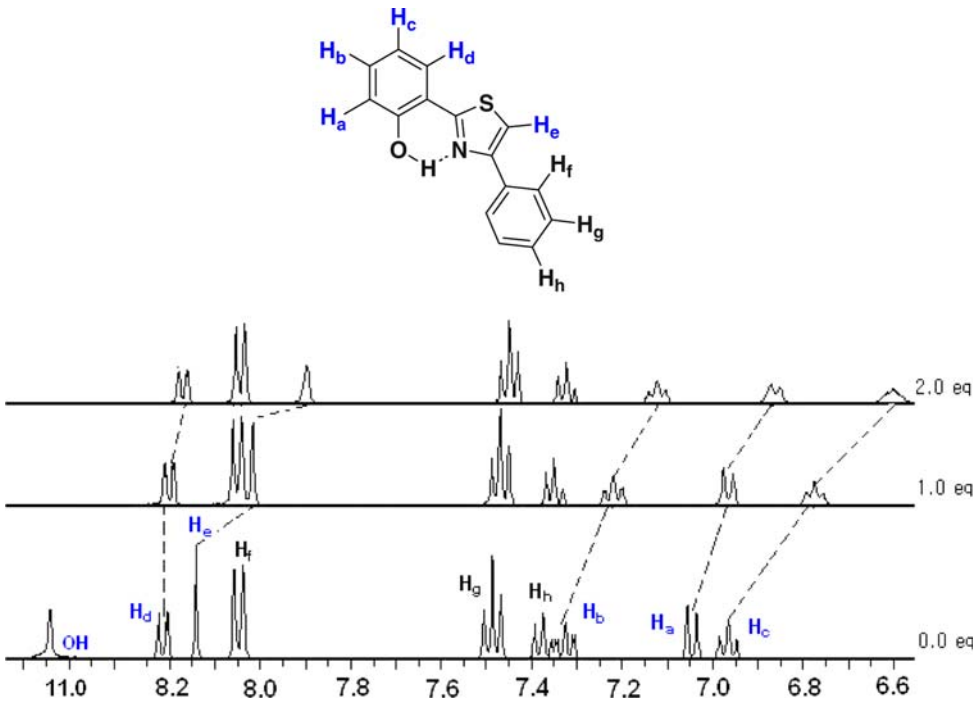

Fig. 5 Partial ^{1}H NMR (400 MHz) spectra of **1** with $[(Bu)_4N]F$ in CD_3CN

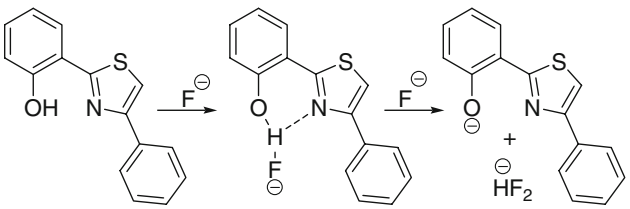

Scheme 3 The mechanism of the interaction of fluoride ions with **1**

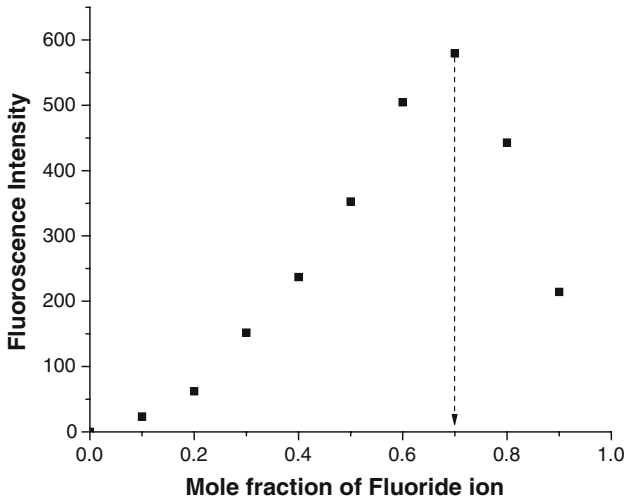

Fig. 6 Job's plot of sensor **1** with F^- in CH_3CN using their fluorescence changes measured at 453 nm

fluoride ion. The acidity of the phenolic proton has been altered by the introduction of electron donating and withdrawing substituents at the *para* position of the phenyl ring. Sensor **2** showed a color change upon addition of fluoride ion and sensor **3** has a higher binding affinity than **1** and **2**.

References

1. Schrader, T., Hamilton, A.D. (eds.): Functional Synthetic Receptors. Wiley-VCH, Weinheim (2005)
2. Stibor, I. (ed.): Anion Sensing. Topics in Current Chemistry, 255, Springer-Verlag, Heidelberg (2005)
3. Martinez-Manez, R., Sancenon, F.: Fluorogenic and chromogenic chemosensors and reagents for anions. Chem. Rev. **103**, 4419–4476 (2003)
4. Sessler, J.L., Davis, J.M.: Sapphyrins: versatile anion binding agents. Acc. Chem. Res. **34**, 989–997 (2001)
5. Kleerekoper, M.: The role of fluoride ion in osteoporosis. Endocrinol. Metab. Clin. North Am **27**, 441–452 (1998)
6. Kirk, K.L.: Biochemistry of the Halogens and Inorganic Halides. Plenum Press, New York (1991)
7. Jung, H.S., Kim, H.J., Vicens, J., Kim, J.S.: A new fluorescent chemosensor for F^- based on inhibition of excited-state intramolecular proton transfer. Tetrahedron Lett. **50**, 983–987 (2009)
8. Cametti, M., Rissanen, K.: Recognition and sensing of fluoride anion. Chem. Commun. 2809–2829 (2009)
9. Grabowski, Z.R., Rotkiewicz, K., Rettig, W.: Structural changes accompanying intramolecular electron transfer: focus on twisted intramolecular charge-transfer states and structures. Chem. Rev. **103**, 3899–4032 (2003)
10. Klymchenko, A.S., Ozturk, T., Pivovarenko, V.G., Demchenko, A.P.: A 3-hydroxychromone with dramatically improved fluorescence properties. Tetrahedron Lett. **42**, 7967–7970 (2001)
11. Klymchenko, A.S., Ozturk, T., Demchenko, A.P.: Synthesis of furanochromones: a new step in improvement of fluorescence properties. Tetrahedron Lett. **43**, 7079–7082 (2002)

12. Rodembusch, F.S., Leusin, F.P., Campo, L.F., Stefani, V.: Excited state intramolecular proton transfer in amino 2-(2′-hydroxyphenyl)benzazole derivatives: effects of the solvent and the amino group position. J. Lumin. **126**, 728–734 (2007)
13. Das, K., Sarkar, N., Ghosh, A.K., Majumdar, D., Nath, D.N., Bhattacharyya, K.: Excited-state intramolecular proton transfer in 2-(2′-hydroxyphenyl)-benzimidazole and -benzoxazole: effect of rotamerism and hydrogen bonding. J. Phys. Chem. **98**, 9126–9132 (1994)
14. Purkayastha, P., Chattopadhyay, N.: Rotamerisation and intramolecular proton transfer of 2-(2′-hydroxyphenyl)oxazole, 2-(2′-hydroxyphenyl)imidazole and 2-(2′-hydroxyphenyl)thiazole: a theoretical study. J. Mol. Struct. **604**, 87–99 (2002)
15. Lee, C., Lee, D.H., Hong, J.I.: Colorimetric anion sensing by porphyrin-based anion receptors. Tetrahedron Lett. **42**, 8665–8668 (2001)
16. Devaraj, S., Saravanakumar, D., Kandaswamy, M.: Dual chemosensing properties of new anthraquinone-based receptors toward fluoride ions. Tetrahedron Lett. **48**, 3077–3081 (2007)
17. Luxami, V., Kumar, S.: Colorimetric and ratiometric fluorescence sensing of fluoride ions based on competitive intra- and intermolecular proton transfer. Tetrahedron Lett. **48**, 3083–3087 (2007)
18. Saravanakumar, D., Devaraj, S., Iyyampillai, S., Mohandoss, K., Kandaswamy, M.: Schiff's base phenol-hydrazone derivatives as colorimetric chemosensors for fluoride ions. Tetrahedron Lett. **49**, 127–132 (2008)
19. Lee, D.H., Lee, H.Y., Lee, K.H., Hong, J.I.: Selective anion sensing based on a dual-chromophore approach. Chem. Commun. 1188–1189 (2001)
20. Desiraju, G.R.: Crystal Design: Structure and Function. Perspectives in Supramolecular Chemistry. Wiley-VCH, England (2002)
21. Bruker.: SHELXTL, Structure Determination Software Programs, Bruker Analytical X-Ray Instruments Inc., Madison, Wisconsin, USA (1997)
22. Bach, T., Heuser, S.: Synthesis of 2-(*o*-hydroxyaryl)-4-arylthiazoles by regioselective Pd (0)-catalyzed cross-coupling. Tetrahedron Lett. **41**, 1707–1710 (2000)
23. Keck, J., Kramer, H.E.A., Port, H., Hirsch, T., Fischer, P., Rytz, G.: Investigations on polymeric and monomeric intramolecularly hydrogen-bridged UV absorbers of the benzotriazole and triazine class. J. Phys. Chem. **100**, 14468–14475 (1996)